https://doi.org/10.5194/egusphere-2026-4653
Preprint. Discussion started: 6 October 2026
© Author(s) 2026. CC BY 4.0 License.

Systematic Evaluation of the Meteosat-12 Lightning Imager Using Direct Lightning Current Measurements from an Instrumented Wind Turbine

Franjo Vukovic[a], Joan Montanya[b], Marcelo Arcanjo[b], Bozidar Filipovic-Grcic[a]

[a]*University of Zagreb Faculty of Electrical Engineering, Zagreb, Croatia*
[b]*Polytechnic University of Catalonia, Barcelona, Spain*
Correspondence: Franjo Vukovic, franjo.vukovic@fer.hr

Abstract

Geostationary optical lightning imagers provide continuous observations of total lightning activity, but their response to upward lightning and continuing-current-dominated flashes remains difficult to evaluate because direct current-based ground truth is rarely available. This paper evaluates Meteosat-12 Lightning Imager (LI) observations using direct lightning-current measurements from an instrumented wind turbine in Croatia. The turbine is equipped with a current-measurement system, and selected events are additionally documented using high-speed video and observations from a ground-based lightning location system. We analyze 76 direct strikes to the instrumented wind turbine during the LI pre and operational period from July 2024 to February 2026. The dataset consists predominantly of upward flashes, with only five downward cloud-to-ground cases, and includes negative, positive, and bipolar flashes. It also encompasses waveform classes dominated by initial continuous current (ICC), as well as flashes containing pulse-type components such as return strokes (RSs). For each measured lightning current waveform, LI group-level observations were extracted within 50 km of the turbine and referenced to the onset and duration of the measured current. LI detections were evaluated in a preceding window, from 500 ms before current onset to the beginning of current flow, and in a during-current window extending over the measured current duration. The overall LI detection efficiency was 76.3 % when detections in either window were considered, with efficiencies of 61.8 % in the preceding window and 65.8 % during the measured current flow. LI detectability depended on current waveform class, with flashes containing pulse-type components generally more frequently detected during current flow. Furthermore, LI detected groups more frequently in the preceding window for positive flashes initiated by negative upward leaders than for their negative-polarity counterparts. In contrast, the detection efficiency during the current-flow window was the same for both polarities. The day/night analysis showed a modestly higher detection efficiency at night. Moreover, group-count, radiance, and flash-level analyses show that LI observations mainly represent the cloud-top optical manifestation of the broader lightning process rather than the local attachment process alone. These results demonstrate the value of direct lightning-current measurements for evaluating satellite optical lightning observations of lightning.

Keywords: initial continuous current; upward lightning; wind turbines; lightning current measurements; Meteosat-12 Lightning Imager; lightning-triggered upward lightning; space-based lightning detection

1. Introduction

The continuous observation of lightning from space has become an increasingly important capability for atmospheric monitoring, severe-weather nowcasting, lightning climatology, and the assessment of lightning-related hazards. In contrast to ground-based lightning location systems (LLSs), which detect electromagnetic emissions produced by lightning discharges, satellite-based optical lightning imagers observe transient optical emissions escaping from clouds and therefore provide a complementary view of total lightning activity. Early satellite observations from the Optical Transient Detector (OTD) and the Lightning Imaging Sensor (LIS) demonstrated the value of optical measurements for mapping lightning occurrence over large regions and for building long-term climatological datasets (Boccippio and Christian, 1998; Christian et al., 1999). More recently, geostationary lightning imagers have enabled continuous monitoring over fixed Earth disks, including the Geostationary Lightning Mapper (GLM) onboard the GOES-R series, the Lightning Mapping Imager onboard the Fengyun-4 series, and the Lightning Imager (LI) onboard Meteosat-12 (Goodman et al., 2013; Hui et al., 2020; Blakeslee et al., 2020; Holmlund et al., 2021). These instruments have substantially expanded the spatial and temporal coverage of lightning observations and are increasingly used in both scientific and operational contexts.

The Meteosat-12 Lightning Imager represents the first European geostationary optical lightning mission. The instrument detects short optical pulses associated with lightning in a narrow spectral band near the neutral oxygen emission line around 777.4 nm, using millisecond-scale sampling and on-board background subtraction to identify lightning-related optical transients (Dobber et al., 2014; Holmlund et al., 2025). LI observations are organized into hierarchical products, including events, groups, and flashes, which provide information on the timing, location, spatial extent, and radiance of optical lightning activity. Since the start of Meteosat-12 LI data dissemination, the instrument has provided continuous observations over Europe, Africa, the Atlantic Ocean, and

https://doi.org/10.5194/egusphere-2026-4653
Preprint. Discussion started: 6 October 2026
© Author(s) 2026. CC BY 4.0 License.

adjacent regions, offering a new capability for monitoring total lightning activity in the European sector (Enno et al., 2025; Bližňák and Sokol, 2026; Viticchié et al., 2026).

Despite this observational capability, satellite lightning measurements require careful evaluation because they do not measure the lightning associated current. Optical emissions observed at cloud top depend not only on the electrical processes occurring within the flash, but also on cloud optical thickness, scattering and absorption, viewing geometry, background illumination, instrument thresholding, and the spatial and temporal clustering algorithms used to produce higher-level products. Consequently, a satellite detection or non-detection cannot be interpreted solely as the presence or absence of lightning current at the ground. Instead, LI observations must be understood as measurements of the optical manifestation of lightning as seen from space. This distinction is particularly important when interpreting flashes that include continuing-type currents, such as initial continuous currents (ICCs) in upward lightning, which may be electrically important at the attachment point but not necessarily optically bright at cloud top.

Most evaluations of satellite lightning imagers have relied on comparisons with other remote-sensing systems, especially ground-based LLSs, VHF lightning mapping systems, and, in some cases, other satellite optical instruments. Such intercomparisons are essential because each system observes a different physical manifestation of lightning. LLSs operating in the LF/VLF range provide accurate timing and geolocation of impulsive discharge processes, particularly cloud-to-ground strokes, and are therefore widely used for operational lightning monitoring and lightning-risk studies. However, their ability to characterize in-cloud activity and continuing-current processes is limited compared with their performance for impulsive events. This complementarity between ground-based electromagnetic observations and space-based optical observations has been emphasized in previous intercomparison studies. Poelman and Schulz (2020) compared EUCLID observations with ISS-LIS optical measurements and showed that the two systems exhibit distinct detection characteristics. Erdmann et al. (2020) compared ISS-LIS, the Meteorage LF network, and the SAETTA Lightning Mapping Array in the northwestern Mediterranean, highlighting that flash duration, spatial extent, altitude, and lightning type influence satellite optical detectability. Figueras i Ventura et al. (2019) further demonstrated the value of combining lightning observations with other atmospheric measurements to interpret lightning initiation and propagation. These studies provide important methodological context for the evaluation of optical lightning observations, while also showing that satellite and ground-based systems should be considered complementary rather than interchangeable.

The need for complementary observations is especially relevant for upward lightning from tall structures and wind turbines. Upward flashes often begin with an upward leader initiated from the structure and can include long ICCs, continuing currents, pulses superimposed on continuing currents, subsequent return strokes, or combinations of these processes (Rakov and Uman, 2003; Montanyà et al., 2014; Rachidi and Rubinstein, 2022). Because many upward flashes are dominated by continuing-type currents, they may be only partially characterized by conventional LLS data, particularly when no strong impulsive component is present. At the same time, these flashes are important for power systems and wind-energy infrastructure because long-duration currents and large charge transfer can contribute to thermal and mechanical stress in lightning protection systems (IEC 61400-24, 2019; CIGRE C4.407, 2013). For this reason, evaluating how LI observes lightning is not only a satellite-validation problem but also a measurement problem relevant to the interpretation of lightning exposure in power-system applications.

Direct lightning-current measurements provide a uniquely valuable reference for evaluating satellite lightning observations. Unlike LLSs, which infer lightning occurrence and location from remotely measured electromagnetic signals, current sensors installed on an instrumented structure directly measure the waveform flowing through the attachment point. These measurements provide flash onset time, duration, polarity, peak current, continuing-current occurrence, and waveform morphology, and therefore offer a physical ground truth that cannot be obtained from satellite observations or LLS data alone. Instrumented towers have shown the value of such measurements for characterizing lightning attachment to tall structures (Rachidi and Rubinstein, 2022), while recent measurements from the Croatian wind-turbine site provide the direct-current dataset used in this study (Vuković et al., 2025a; Vuković et al., 2026a).

Previous space-based optical studies have also shown that satellite imagers can provide information about flash development that is not available from LLS observations alone. Simultaneous observations from ASIM, ISS-LIS, GLM, ground-based optical systems, and LLSs have demonstrated that optical satellite detections may be associated with different stages of the flash, including in-cloud development, impulsive processes, and continuing-current-related luminosity (van der Velde et al., 2020; Montanyà et al., 2021; Montanyà et al., 2022). These studies motivate the present evaluation of Meteosat-12 LI using direct current measurements as the primary reference, with LLS observations used as complementary context.

Recent work has begun to evaluate Meteosat-12 LI performance using regional ground-based lightning datasets. Bližňák and Sokol (2026) presented an early validation of LI observations using the Earth Networks Total Lightning Network. Gedik et al. (2025) evaluated LI performance over Switzerland and Austria relative to

https://doi.org/10.5194/egusphere-2026-4653
Preprint. Discussion started: 6 October 2026
© Author(s) 2026. CC BY 4.0 License.

ALDIS/BLIDS, reporting different detection behaviour in nationwide datasets and in regions near tall structures where upward lightning is more frequent. Enno et al. (2025) summarized first-year Meteosat-12 LI observations and main performance characteristics. More recently, Viticchié et al. (2026) assessed Meteosat-12 LI detection efficiency using multiple reference systems, including GLD360, EUCLID, and GLM. These studies provide the first broad evaluation of LI performance and establish a valuable baseline for interpreting LI data. However, most available evaluations are still based on comparisons with remote-sensing reference systems. Such comparisons do not provide direct information on the current waveform at the attachment point, and therefore cannot fully assess how LI responds to such flashes.

The present work addresses this gap by evaluating Meteosat-12 LI observations using direct lightning-current measurements from an instrumented wind turbine in Croatia. The site is equipped with low- and high-frequency Rogowski coils installed at the base of the turbine tower, allowing both continuing-type currents and pulse-type currents to be measured. A high-speed camera provides independent optical evidence for selected events when visibility conditions permit, while a regional ground-based LLS supplies complementary information on nearby cloud-to-ground and intracloud detections. In this configuration, the current measurement is used as the primary ground truth for flash occurrence, timing, duration, polarity, and waveform classification; the LLS is used as contextual information on impulsive activity in the surrounding region; and the high-speed video is used as supporting evidence in selected case studies. The authors have already conducted several similar smaller-scale studies (covering a couple of events) in which LI detections were analyzed at a high level for several cases (Vuković et al., 2025b; Vuković et al., 2026b). In this paper, we aim to create robust, reliable statistics over a long-term, multi-month period, across a wider range of lightning conditions, in order to quantify LI performance validated against the absolute ground truth of local measurements.

The analyzed dataset in this paper covers the entire Meteosat-12 LI operational period from July 2024 to February 2026 and includes 76 directly measured lightning-current waveforms at the instrumented wind turbine. The events include different polarities and waveform classes, including ICC-only flashes and flashes containing pulse-type current components. For each measured waveform, LI group-level observations are evaluated relative to the onset and duration of the directly measured current, allowing LI performance to be assessed as a function of current-based flash properties.

The objectives of this paper are therefore to quantify Meteosat-12 LI detection performance for current-measured upward lightning, to evaluate how LI observations differ among current-based flash classes, to examine LI activity preceding the onset of current at the turbine, and to interpret representative events using LI groups, integrated radiance, current waveforms, LLS detections, and high-speed video where available. By using direct lightning-current measurements as the primary reference, this study complements previous LI and ISS-LIS evaluations based mainly on LLS and optical intercomparisons and provides a physically grounded assessment of Meteosat-12 LI observations for lightning affecting wind-energy infrastructure.

2. Methods

2.1 Instrumented Wind Turbine Site and Ground-Based Measurements

The wind farm lightning observatory is located in southern Croatia, near the Adriatic coast, in mountainous terrain. The wind farm consists of 14 wind turbines distributed in two groups of seven, with the eastern group located at generally higher elevations. The instrumented turbine, WT4, is located in this higher-elevation sector at approximately 1250 m above sea level. All turbines have 80 m towers and 49 m blades, corresponding to a maximum blade-tip height of approximately 132 m above ground level. Figure 1 shows the wind-farm layout, including WT4 and the substation where the high-speed camera is installed.

https://doi.org/10.5194/egusphere-2026-4653
Preprint. Discussion started: 6 October 2026
© Author(s) 2026. CC BY 4.0 License.

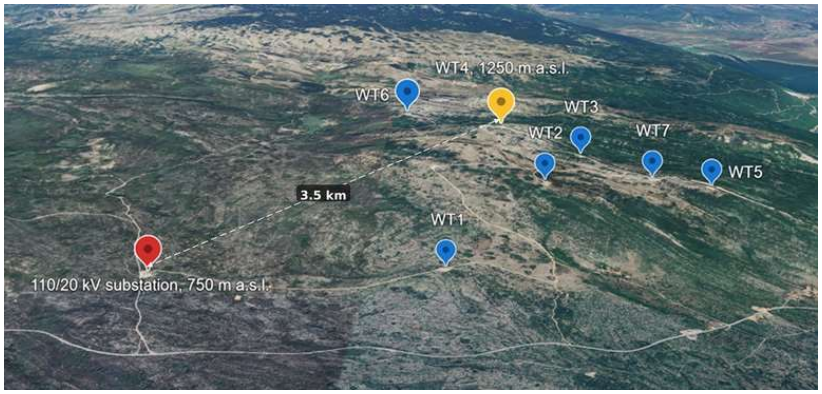

Figure 1. Wind farm layout: substation with high-speed camera and WT4 instrumented with Rogowski-coils.

WT4 has been instrumented since July 2022 with two Rogowski-coil current sensors mounted around the tower near its base, approximately 1 m above ground level. These sensors are used to measure electrical currents that flow through the tower when the wind turbine is struck by lightning. The low-frequency sensor is used to measure continuing-type currents, including ICCs and continuing currents (CCs), whereas the high-frequency sensor is used to measure pulse-type currents, such as return strokes and pulses superimposed on continuing current (Vukovic et al., 2025, 2026).

A high-speed camera installed approximately 3.5 km from WT4, provides supporting optical observations of the instrumented turbine when visibility conditions allow. WT4 is the only turbine within the camera field of view. The camera records approximately 1 s per event, including about 0.2 s of pre-trigger data, with frame rates adjustable from several thousand frames per second up to several tens of thousands of frames per second and a spatial resolution of 640 × 600 pixels. These video observations are not used to define LI detection efficiency, but they are used as independent supporting evidence in selected event-level analyses. The current measuring system and high speed camera installation are shown in Figure 2.

Figure 2a. Rogowski-coil current sensors at the WT4 tower

Figure 2b. High-speed camera

The site is also covered by a regional ground-based VLF/LF Lightning Location System (LLS). The LLS provides information on nearby cloud-to-ground strokes and intracloud detections, including detection time, location, polarity, and classification where available. In this paper, LLS data are used as contextual information on impulsive lightning activity occurring before and during the current-measured flashes.

2.2 Meteosat-12 Lightning Imager (LI)

The LI is an optical lightning sensor composed of four cameras with on-board real-time processing. The instrument detects lightning-related optical transients associated with total lightning activity and converts these detections into higher-level lightning products. The LI field of view covers approximately 84 % of the Earth disk, as shown in Supporting Information on Figure S1a. The spatial sampling is 4.5 km at the sub-satellite point and increases with distance from this point; over central Europe, the effective spatial resolution is approximately 7 km

https://doi.org/10.5194/egusphere-2026-4653
Preprint. Discussion started: 6 October 2026
© Author(s) 2026. CC BY 4.0 License.

(Supporting Information, Figure S1b). The temporal sampling, corresponding to the integration time of each acquisition frame, is 1 ms.

LI primarily detects luminosity escaping from clouds after scattering and absorption by cloud particles. Therefore, LI observations should be interpreted as cloud-top optical measurements of the lightning process rather than as direct measurements of the lightning current. In this study, the LI product used for the statistical analysis is the LI Group (LGR). An LI group is formed from spatially connected lightning events detected within the same 1 ms acquisition frame. Each LGR contains a timestamp, geographic coordinates, and a radiance value. These quantities are used to evaluate the timing, distance, and optical intensity of LI detections relative to the directly measured current waveform at the wind turbine.

Although LI groups can be temporally and spatially clustered into LI flashes, the LI Flash product is not used as the primary product in this paper. The group-level product was selected because it preserves the millisecond-scale timing needed to compare satellite optical detections with the onset and evolution of directly measured current waveforms. The relationship between LI events, groups, and flashes is described in the Supporting Information, Figure S2 and Figure S3.

2.3 LI-Flash identification

For each lightning-current waveform measured at the instrumented wind turbine, LI groups were extracted using criteria referenced to the directly measured current. The onset of the current waveform was used as the reference time, (t = 0), and all LI group times were expressed relative to this onset.

LI groups were selected if they occurred within 50 km of the wind turbine and within the interval from 500 ms before current onset to the end of the measured current waveform. This interval was divided into two windows: a preceding window, from t = -500 ms to t = 0, and a during-current window, from t = 0 to the end of the measured current. The preceding window was used to examine optical activity before current flow at the turbine, while the during-current window was used to evaluate LI detections during the measured electrical current flow.

The 50 km radius was selected to include optical activity near the turbine as well as nearby or parent-flash activity that may be physically related to the current-measured event. The 500 ms preceding window was selected to capture optical activity shortly before current onset while limiting unrelated storm activity. Therefore, preceding LI activity is interpreted as temporally and spatially associated with the current-measured event, but not by itself as definitive evidence of triggering.

LI detection was evaluated separately in the preceding and during-current windows. A detection was defined as the presence of at least one LI group in the corresponding window. The overall LI detection efficiency was defined as the fraction of current-measured flashes with at least one LI group in either window.

2.4 Derived LI Metrics and Flash-Level Visualizations

For each current-measured flash, LI-based metrics were derived separately for the preceding and during-current windows. The primary metric was the LI detection status, defined by the presence or absence of at least one LI group in the corresponding window. In addition, the number of LI groups was counted in each window to quantify the amount of detected optical activity associated with each current-measured event.

Radiance statistics were calculated from the LI group radiance values. For each flash and each analysis window, the median radiance of all detected LI groups was computed. Class-level radiance statistics were then calculated from these per-flash median values, rather than from all LI groups pooled together. This approach prevents flashes with many detected groups from dominating the statistics. Median radiance was used as the primary radiance metric because LI radiance distributions are skewed and may include isolated high-radiance groups.

For flashes with LI detections in the preceding window, two additional quantities were extracted. The earliest preceding LI group was defined as the first LI group detected within that window. The closest preceding LI group was defined as the LI group with the smallest horizontal distance to the wind turbine within the same window. For both quantities, the time relative to current onset, horizontal distance from the turbine, and radiance were recorded.

For selected flash-level analyses, LI groups were visualized using longitude-latitude maps centered on the wind turbine and time-distance plots referenced to the current onset. An integrated LI radiance time series was also calculated by summing the radiance of all LI groups detected within each 1 ms acquisition frame and within the 50 km spatial window. This integrated radiance was compared with the directly measured current waveform, and with LLS detections and high-speed video observations when available.

https://doi.org/10.5194/egusphere-2026-4653
Preprint. Discussion started: 6 October 2026
© Author(s) 2026. CC BY 4.0 License.

3. LI Detection Performance

The results are organized to evaluate Meteosat-12 LI observations with respect to the directly measured lightning-current waveforms at the instrumented wind turbine. First, the current-measured dataset is summarized in terms of flash occurrence, polarity, waveform components, and duration. The LI detection performance is then quantified using the two analysis windows defined in Section 2.3: the preceding window, from 500 ms before current onset to the beginning of the measured current, and the during-current window, from current onset to the end of the measured current. Finally, the LI response is examined in terms of detection efficiency, number of detected LI groups, group radiance, preceding optical activity, and day/night observing conditions.

3.1 Current-measured dataset and flash classification

Figure 3 summarizes the lightning-current waveform dataset collected between July 2024 and February 2026. During this period, 76 lightning current waveforms were recorded at the instrumented wind turbine using the Rogowski-coil measurement system. The monthly distribution is consistent with the longer-term behaviour observed at the site since the installation of the measurement system in July 2022: most flashes occurred during winter and transitional months, whereas summer activity was limited. When interpreting the seasonal distribution, it should be noted that the dataset includes two winters, two summers, and two autumns, but only one spring. The day/night occurrence was approximately balanced, with 39 flashes recorded during daytime and 37 at night.

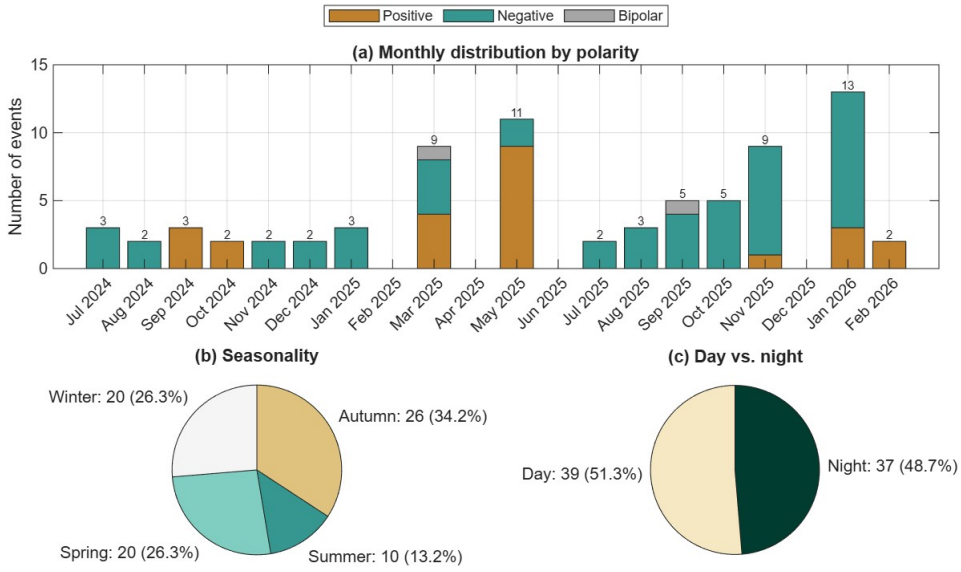

Figure 3. Dataset overview: monthly and seasonal flash occurrence, polarity, and day/night distribution

Figure 4 presents the current-based classification of the dataset. The flashes were classified according to polarity and waveform components, including the presence or absence of ICCs, RSs, and pulses superimposed on continuing current (SIs). The dataset is dominated by upward flashes, which account for 93 % of the events during the study period; only five downward flashes were recorded. Considering all flashes, 65.8 % were negative, 31.6 % were positive, and 2.6 % were bipolar. ICC-only upward flashes represented 57.9 % of the full dataset. Within this ICC-only subset, the polarity distribution was approximately balanced, with 47.7 % positive and 52.3 % negative events.

https://doi.org/10.5194/egusphere-2026-4653
Preprint. Discussion started: 6 October 2026
© Author(s) 2026. CC BY 4.0 License.

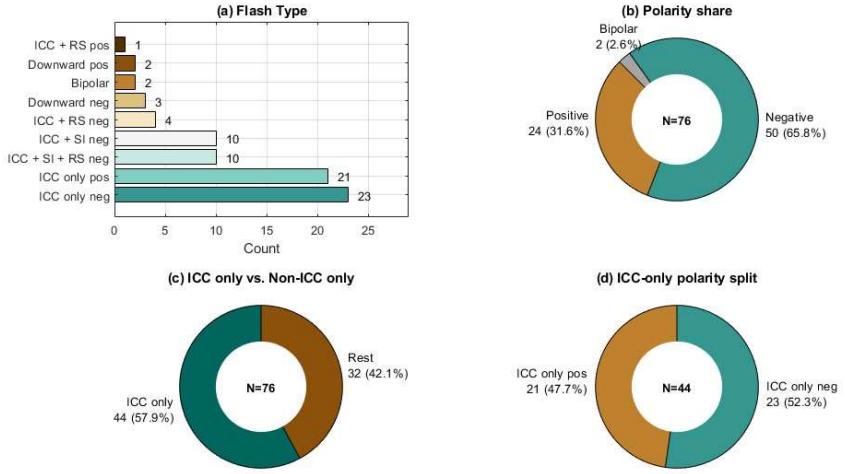

Figure 4. Dataset overview: flash-type classification based on current components, overall polarity distribution, ICC-only versus non-ICC, and the polarity split within the ICC-only subset

Table 1 lists the mean flash duration for the considered splits: positive vs. negative, ICC-only positive vs. ICC-only negative, and ICC-only vs. non-ICC-only (rest) flashes. The average durations of negative flashes are substantially longer than those of positive flashes, both when considering the full polarity-based subset and when the analysis is restricted to ICC-only flashes.

Table 1 Average flash duration by polarity and type classification

Flash type	Average duration
Positive	0.064 s
Negative	0.256 s
ICC-only positive	0.061 s
ICC-only negative	0.152 s
ICC-only	0.108 s
Non-ICC-only	0.318 s

3.2 Overall LI detection performance

For each current-measured flash, LI groups were searched within 50 km of the instrumented wind turbine and within the temporal interval extending from 500 ms before current onset to the end of the measured current. A flash was considered detected by LI if at least one LI group was found either in the preceding window, in the during-current window, or in both windows.

Figure 5 shows the LI detection efficiency stratified by current-based flash type. Figure 5a presents the overall detection efficiency, defined as the percentage of flashes with at least one LI group in the preceding window and/or during-current window. Figure 5b separates the detections into four categories: preceding window only, during-current window only, both windows, and no LI detection.

The total dataset contains N = 76 flash events based on the measured currents on the instrumented wind turbine. The overall LI detection efficiency is 76.3 % when considering at least one LGR detection in either the preceding or during window. When the two windows are considered separately, the detection efficiency is 61.8% for the preceding window and 65.8 % for the during window. In the preceding window, this means that in roughly 62% of cases, the LI detected activity prior to the flash, which may indicate an association with the triggering process. Confirming this will require further analysis in future work, incorporating additional observations and measurement techniques to corroborate the finding and strengthen its reliability. For the remaining flashes, the

https://doi.org/10.5194/egusphere-2026-4653
Preprint. Discussion started: 6 October 2026
© Author(s) 2026. CC BY 4.0 License.

events may have been self-initiated, or the optical activity associated with in-cloud leaders that potentially contributed to triggering may have been too weak, too obscured and as such outside the LI detection capability.

In general, according to Figure 5, the results demonstrate that flashes are usually always detected when they contain pulse-type currents, such as RSs. This is expected, as these events produce the most intense optical emissions, allowing them to emerge above the cloud top, either from the channel below the cloud or from related IC activity. In cases involving only ICC, or ICC accompanied by low-intensity SIs, the detection efficiency decreases. Based on Figure 5, it is clear that negative ICC-only flashes and negative ICC + SI flashes are the categories most frequently missed by the LI. The ICC + SI category exhibits a bit lower detection rate than the ICC-only negative flashes. This can be explained by the fact that ICC + SI flashes are often more similar to ICC-only flashes, owing to the relatively low-amplitude pulses they may contain, in contrast to ICC + RS flashes, which include intensive RSs.

Optical emissions from the channel segment below the cloud during ICC flow are not expected to be intense enough to penetrate optically thick clouds and reach the LI. Therefore, detections in these cases are more likely associated with lightning activity occurring within the cloud before or during the flash.

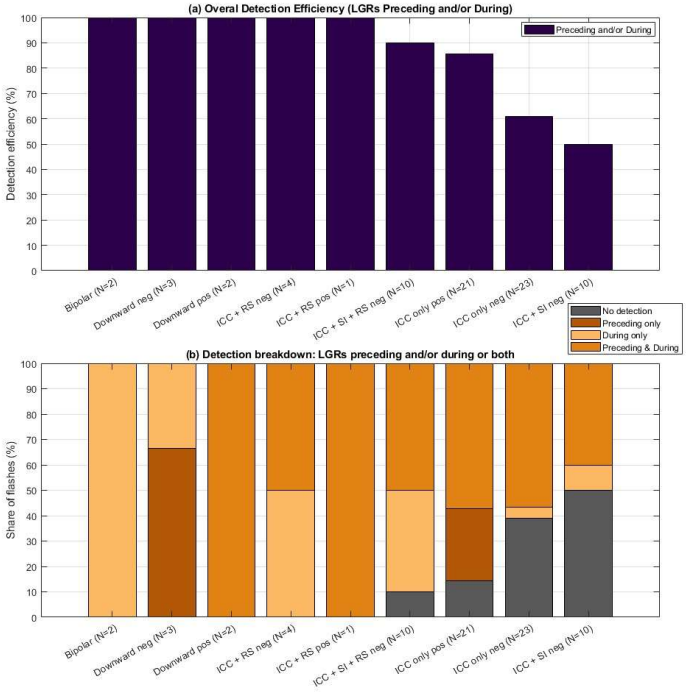

Figure 5. LI detection efficiency by flash type: a) Overall detection efficiency (preceding and/or during window); b) Detailed breakdown by LI detection window preceding-only, during-only, and both windows

3.3 Detection efficiency as a function of current waveform class

Figure 6 shows the detection efficiency for preceding activity only, during-flash LI activity only, and combined efficiency (preceding or during), for three comparison scenarios: (a) positive vs. negative flashes, (b) ICC-only positive vs. ICC-only negative flashes (to eliminate, or at least partially mitigate the potential impact of pulse-type currents on detection efficiency when comparing polarities), and (c) ICC-only vs. non-ICC-only flashes (to analyze the potential impact of pulse-type currents on detection efficiency).

When comparing positive and negative flashes, as shown on Figure 6a, it can be seen that, for LGRs detected during lightning current flow through the WT, the detection efficiency is approximately the same for positive (63 %) and negative (66 %) flashes. However, the most notable difference appears in the preceding activity, 87.5 % for positives vs 52 % for negatives, which may provide insight into triggering mechanisms and related IC activity.

To reduce the influence of pulse-type currents on the polarity comparison, Figure 6b restricts the analysis to ICC-only positive and ICC-only negative flashes. The same tendency remains evident. ICC-only positive flashes

https://doi.org/10.5194/egusphere-2026-4653
Preprint. Discussion started: 6 October 2026
© Author(s) 2026. CC BY 4.0 License.

show substantially higher preceding-window detection efficiency than ICC-only negative flashes, 85.7 % compared with 56.5 %, whereas the during-current detection efficiency is more similar between the two classes. This indicates that the polarity dependence observed in the preceding window is not caused only by the presence of return strokes or other strong impulsive current components. When comparing ICC-only positives and ICC-only negativ, triggered positive ICCs are expected to be more strongly influenced by the negative charge region involved in the upward/triggering process than by the lower positive charge pocket. This suggests that the higher detection efficiency for triggered positive ICCs arises because their optical emissions originate nearer the cloud top, at the negative charge region, where photons encounter less optical thickness from the overlying cloud layers and can therefore reach the LI more easily.

Figure 6c compares ICC-only flashes with non-ICC-only flashes. During the measured current flow, the detection efficiency is higher for non-ICC-only flashes, consistent with the presence of pulse-type current components that can produce stronger optical emissions. In contrast, for the preceding window alone, the detection efficiency is higher for ICC-only flashes than for non-ICC-only flashes. This result suggests that the preceding-window and during-current-window detections contain different information: the preceding window is more sensitive to optical activity associated with the parent or nearby in-cloud discharge before current onset at the turbine, whereas the during-current window is more strongly influenced by the current waveform structure and the presence of impulsive components.

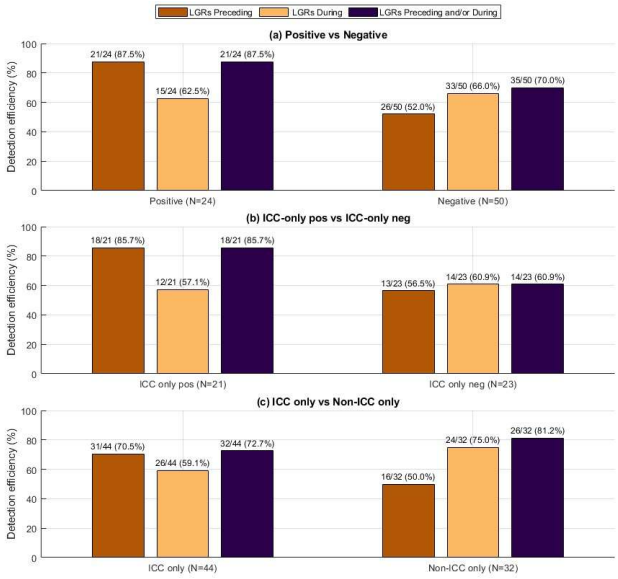

Figure 6. Detection efficiency comparison for positive vs. negative flashes, ICC-only positive vs. ICC-only negative flashes, and ICC-only vs. non-ICC-only flashes

3.4 Number of detected LI groups

Figure 7 shows boxplots of the number of LI LGRs for flashes with detections in the preceding (top row) and during-flash (bottom row) windows. The red line denotes the median and × denotes the mean. The box spans from the 25th percentile to the 75th percentile, and whiskers extend to the most extreme values within 1.5×IQR (only to the most extreme non-outlier values).

When analysing polarity, the median number of LI LGRs is higher for negative than for positive flashes in both the preceding and during-flash windows. The mean number of LGRs is also higher for negative flashes during the flash, whereas in the preceding window the mean values for positive and negative flashes are very similar, with a slightly higher value for positive flashes. The same trend is more clearly observed when considering only ICC-only flashes: ICC-only negative flashes show higher median and mean LGR counts than ICC-only positive flashes in both windows. Overall, the median is more stable than the mean; across windows and regardless of whether pulse-type currents are present, negative flashes typically exhibit a median LGR count about two to three times

https://doi.org/10.5194/egusphere-2026-4653
Preprint. Discussion started: 6 October 2026
© Author(s) 2026. CC BY 4.0 License.

that of positive flashes. The higher number of LGRs detected during the flash in negative cases is consistent with the generally longer duration of negative flashes. For positive flashes, the preceding window shows a wider range of LGR counts, including the highest observed value.

When comparing ICC-only flashes with non-ICC-only flashes, it is noteworthy that in the preceding window the LI detects more LGRs for ICC-only flashes, both in terms of the mean and the median LGR count. In contrast, during the flash, the medians are broadly similar for ICC-only and non-ICC-only flashes, whereas the mean LGR count is higher for non-ICC-only flashes (i.e., flashes that include pulse-type currents) than for ICC-only flashes.

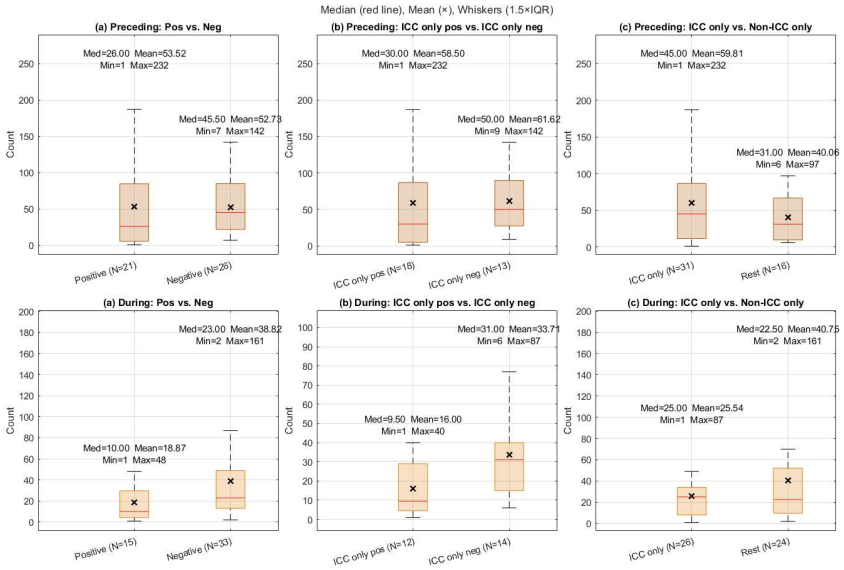

Figure 7. Detected flash events: boxplots of LI LGR counts in the preceding and during-flash windows (positive vs. negative, ICC-only positive vs. ICC-only negative, and ICC-only vs. non-ICC-only).

In the Supporting Information, for each lightning flash case, the flash duration and the number of LGRs detected in the preceding window and in the during-the-flash window are presented (Figure S4). Each column corresponds to one split: positive vs. negative, ICC-only positive vs. ICC-only negative, and ICC-only vs. non–ICC-only flashes. The figure also enables inspection of flash-duration tendencies for the different categories. In particular, negative flashes generally last longer than positive flashes which may be important aspect when considering the number of LGRs detected.

3.5 LI group radiance statistics

Figure 8 shows boxplots of median LGR radiance in the preceding and during-flash windows for positive vs. negative flashes, ICC-only positive vs. ICC-only negative flashes, and ICC-only vs. non-ICC-only flashes. For each LI-detected event, the median radiance across all detected LGRs was computed separately for the preceding and during windows and shown against flash duration (Supporting Information, Figure S5), similar to Figure S4. These per-event median radiances were then summarized across events within each class. Thus, the reported radiance statistics are based on the median LGR radiance of each individual event, rather than on all LGRs pooled together. This approach prevents events with large numbers of detected LGRs from disproportionately influencing the class-level statistics. Furthermore, median radiances are used throughout the analysis because the LI radiance distributions are highly skewed and occasionally contain very high-radiance cases. Therefore, the median provides a more robust and representative measure of the typical radiance than the mean.

When considering all positive and negative cases, the preceding-window median radiance is slightly higher for positive than for negative flashes. However, negative flashes exhibit higher during-window median radiance values, which is consistent with the presence of intense pulse-type components, including RSs, in many negative flashes.

When the analysis is restricted to ICC-only flashes, the separation in preceding-window median radiance becomes more pronounced in favour of ICC-only positive flashes. Moreover, in the during-flash window the trend

https://doi.org/10.5194/egusphere-2026-4653
Preprint. Discussion started: 6 October 2026
© Author(s) 2026. CC BY 4.0 License.

reverses compared with the full positive/negative comparison: ICC-only positive flashes (associated with negative upward leaders) exhibit higher median radiance than ICC-only negative flashes (associated with positive upward leaders). This indicates that the higher radiance observed for negative flashes in the full dataset is largely driven by pulse-type components (e.g., RSs and ICC pulses). Once these components are excluded, the optical signature appears to be dominated by the upward leader development and/or associated IC activity, suggesting that negative upward leaders may be optically brighter and/or less attenuated than positive upward leaders.

Furthermore, a plausible interpretation is related to cloud attenuation and charge-layer distribution inside the cloud. Negative upward leaders from the WT are typically triggered by in-cloud activity involving the upper charge region, so the optical emission from the leader near the turbine tip may experience less attenuation. In contrast, upward positive leaders can be linked to activity involving lower charge regions, where a larger fraction of the luminous channel may be embedded deeper in cloud, increasing attenuation by cloud particles.

Figure 8 also compares ICC-only versus non-ICC-only flashes. In the preceding window, non-ICC-only flashes tend to exhibit higher median radiance than ICC-only flashes. During the flash window, the difference becomes more pronounced, with non-ICC-only flashes showing substantially higher median radiance. This is consistent with the strong optical emissions associated with pulse-type currents, particularly RSs.

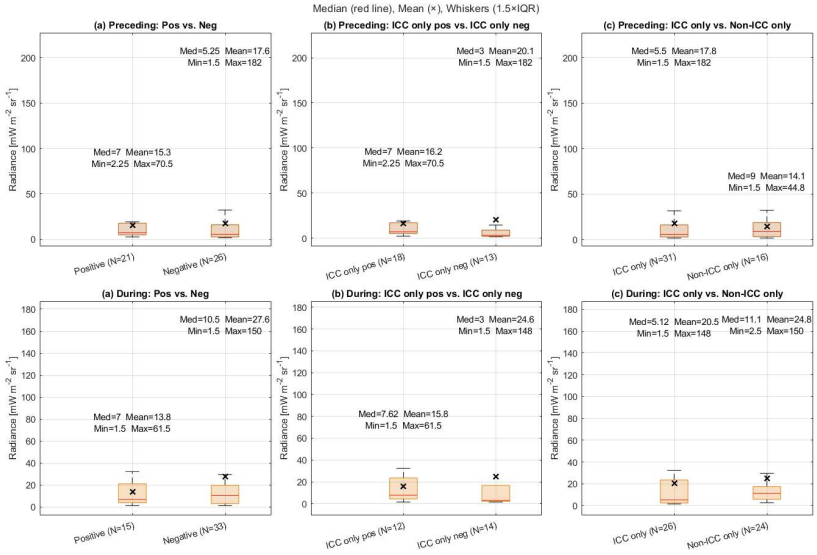

Figure 8. Radiance statistics (median and mean) of LI LGRs in preceding and during-flash windows: positive vs. negative, ICC-only positive vs. ICC-only negative, and ICC-only vs. non-ICC-only flashes

3.6 LI activity preceding current onset

Figure 9 shows, for each flash detected in the preceding window, the earliest LI-detected LGRs plotted as detection time (Δt before onset) versus distance from the wind turbine. In Figure 9, cases are colored using categorical coloring for positive vs. negative (Figure 9a), and ICC-only positive vs. ICC-only negative flashes (Figure 9b). Table 2 provides detailed statistics on the detection timing, distance from the instrumented WT, and radiance of the earliest detected groups for all flashes and for the same classifications.

The earliest groups shown in Figure 9 are interpreted as signatures of other lightning processes occurring prior to the measured current onset, which may have contributed to initiating the wind-turbine lightning flashes. Considering all earliest detected preceding groups, regardless of flash type (N = 47), the Δt (earliest LGR time) has a median/mean of 0.2446/0.2498 s. The corresponding distance has a median/mean of 19.65/21.47 km, and the radiance has a median/mean of 8/12.15 mW m^{-2} sr^{-1}, respectively.

Regarding the average time (mean time) of earliest LGRs before flash onset, there appears to be no difference between positive and negative flashes, between ICC-only positive and ICC-only negative flashes, or between ICC-only and non-ICC-only flashes (Table 2). However, the earliest detected groups associated with negative flashes usually occur at larger distances, with a median/mean of 24.950/26.537 km, whereas the earliest groups

https://doi.org/10.5194/egusphere-2026-4653
Preprint. Discussion started: 6 October 2026
© Author(s) 2026. CC BY 4.0 License.

associated with positive flashes are primarily found at shorter distances, with a median/mean of 13.852/15.188 km (including cases within ~10 km). In this dataset, no earliest groups associated with positive flashes are observed beyond ~35 km, and no earliest groups associated with negative flashes are observed within ~10 km (Figure 9a-b). The same pattern is observed when comparing ICC-only positive and ICC-only negative flashes (Table 2). In contrast, when comparing ICC-only and non-ICC-only flashes, there appear to be virtually no differences: the ICC-only subset has a median/mean distance of 19.52/21.25 km, while the non-ICC-only subset has a median/mean distance of 21.67/21.89 km, according to Table 2. Additional details are provided in the Supporting Information on Figure 6Sd, where the data for ICC-only and non-ICC-only flashes are shown in a format similar to Figure 9a–b, together with an additional distance–time visualization in which all events are colored by radiance Supporting Information on Figure S6a.

The earliest LI LGRs associated with positive flashes exhibit slightly higher radiances, both in terms of mean and median values, than those associated with negative flashes, as shown in Table 2. This trend remains evident when pulse-type currents are excluded and only ICC-only positive and ICC-only negative flashes are compared (Table 2). In the comparison between ICC-only and non-ICC-only flashes, the earliest pre-triggering LGRs associated with non-ICC-only flashes also appear to exhibit slightly higher radiances (Supporting Information, Figure S6d). This tendency is generally consistent when all pre-trigger LGRs, rather than only the earliest ones, are considered on a flash-by-flash basis over the entire preceding window (see previous Figure 8a–c). The median of the flash-level median radiances over the entire preceding window remains higher for positive flashes than for negative flashes (7.00 vs. 5.25 mW m^{-2} sr^{-1}), and the same tendency is observed for ICC-only positive and ICC-only negative flashes (7.00 vs. 3.00 mW m^{-2} sr^{-1}). However, the corresponding mean values of the flash-level median radiances are higher for negative flashes than for positive flashes (17.56 vs. 15.26 mW m^{-2} sr^{-1}) and for ICC-only negative flashes than for ICC-only positive flashes (20.06 vs. 16.15 mW m^{-2} sr^{-1}), indicating the influence of a limited number of high-radiance negative cases. Therefore, the median-based statistics are considered more representative for this dataset.

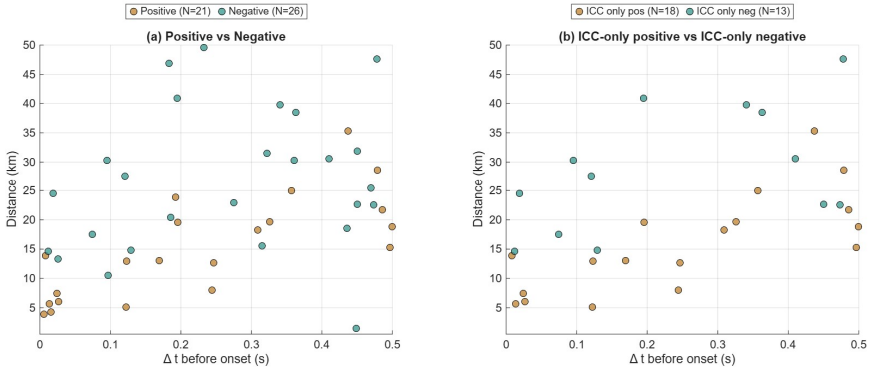

Figure 9. Earliest LI-detected LGRs in the preceding window: detection time versus distance from the wind turbine for positive vs. negative, ICC-only positive vs. ICC-only negative, and ICC-only vs. non-ICC-only flashes.

Table 2 Earliest detected LI LGRs statistics in the preceding-activity window for the entire dataset and per flash type (ICC-only positive vs. ICC-only negative, and ICC-only vs. non-ICC-only flashes)

Group	N	Δt before flash (s) (median/mean)	Distance (km) (median/mean)	Radiance (mW m^{-2} sr^{-1}) (median/mean)
All	47	0.245 / 0.250	19.650 / 21.466	8.000 / 12.149
Pos	21	0.196 / 0.228	13.852 / 15.188	9.000 / 12.714
Neg	26	0.295 / 0.268	24.950 / 26.537	7.000 / 11.692
ICC-only pos	18	0.246 / 0.254	14.578 / 15.936	7.500 / 13.694
ICC-only neg	13	0.195 / 0.243	27.569 / 28.604	3.500 / 9.269
ICC-only	31	0.245 / 0.249	19.524 / 21.248	6.000 / 11.839
Non-ICC-only	16	0.254 / 0.251	21.671 / 21.887	8.750 / 12.750

https://doi.org/10.5194/egusphere-2026-4653
Preprint. Discussion started: 6 October 2026
© Author(s) 2026. CC BY 4.0 License.

In addition to the earliest groups, it is also useful to analyze the LI groups occurring closest to the measured current within the preceding window. Table 3 provides detailed statistics on the detection timing, distance from the instrumented WT, and radiance of the closest detected groups for all flashes and for the same classifications used previously: positive vs. negative, ICC-only positive vs. ICC-only negative, and ICC-only vs. non-ICC-only. Additional visualizations, analogous to those previously presented for the earliest detected group, are provided in the Supporting Information on Figure S7, where the closest LI-detected LGRs for each flash detected within the preceding time window are plotted as detection time, Δt before onset, versus distance from the wind turbine. When the closest preceding LI LGRs are considered, their distances are generally smaller than those of the earliest preceding LGRs, as expected. The results indicate that the closest groups are most commonly detected at distances on the order of ~5–10 km from the instrumented WT (median distance), with lower values associated with positive flashes (~5 km) and higher values associated with negative flashes (~10 km). The same trend is observed when comparing ICC-only positive and ICC-only negative flashes (Table 3). For all flashes combined, the occurrence time of the closest groups has a median/mean of 0.038/0.080 s, and it is broadly similar when comparing the positive and negative subsets (Table 3). However, when comparing ICC-only positive and ICC-only negative flashes, the closest groups for ICC-only negative flashes occur temporally closer to flash onset, with a median lead time of ~22 ms, in contrast to ICC-only positive flashes (~50 ms) (Table 3). In conclusion, a considerable number of flashes exhibit closest groups detected within only a few kilometers of the turbine and tens of milliseconds prior to onset, suggesting very late-stage activity immediately preceding initiation.

A plausible interpretation, based on the combination of the information related on the earliest groups (Figure 9, Table 2 and Supporting Information Figure S6a), where the earliest groups are dispersed over relatively large distances of up to approximately 50 km, and information related to the closest groups (see Table 3 and Supporting Information Figure S7a) where they are concentrated near the instrumented WT and may correspond to the latest LGR groups in the preceding activity, is that these signatures may reflect in-cloud leader activity that initially develops at larger distances and then propagates toward the turbine. Such a progression could create favorable conditions for the initiation of either negative or upward positive leaders from the WT by redistributing charge within the cloud and establishing a charge configuration favorable for upward leader development.

Finally, the median and mean radiances of the closest groups are higher than those of the earliest groups when considering all flash types together (Table 2 vs. Table 3, first row). The difference is marginal for the median radiance, whereas it is more pronounced for the mean radiance.

Table 3 Closest detected LI LGRs statistics in the preceding-activity window for the entire dataset and per flash type (ICC-only positive vs. ICC-only negative, and ICC-only vs. non-ICC-only flashes)

Group	N	Δt before (s) (median/mean)	Distance (km) (median/mean)	Radiance (median/mean)
All	47	0.038 / 0.080	8.162 / 9.033	8.500 / 58.223
Pos	21	0.038 / 0.076	5.091 / 7.516	9.000 / 25.667
Neg	26	0.040 / 0.083	9.454 / 10.258	3.750 / 84.519
ICC-only pos	18	0.051 / 0.084	5.810 / 7.990	9.500 / 26.528
ICC-only neg	13	0.022 / 0.053	10.464 / 8.300	2.000 / 158.423
ICC-only	31	0.038 / 0.071	7.970 / 8.120	8.500 / 81.839
Non-ICC-only	16	0.040 / 0.096	8.961 / 10.801	8.000 / 12.469

3.7 Day/night dependence of LI observations

The dataset was also separated into daytime and nighttime events to evaluate whether background illumination affects LI detection performance and radiance statistics. Figure 10a shows the day/night distribution by flash type. The full dataset is approximately balanced between daytime and nighttime events, with 39 flashes occurring during the day and 37 at night. However, the flash-type composition is not identical in the two subsets. During the day, negative flashes account for 24 out of 39 events, positive flashes for 13 events, and bipolar flashes for 2 events. At night, negative flashes account for 26 out of 37 events, positive flashes for 11 events, and no bipolar flashes are present. In addition, ICC-only negative flashes occur more frequently at night than during the day. This uneven composition must be considered when interpreting the day/night comparison.

https://doi.org/10.5194/egusphere-2026-4653
Preprint. Discussion started: 6 October 2026
© Author(s) 2026. CC BY 4.0 License.

Figure 10b shows the LI detection efficiency separated into daytime and nighttime cases, including the preceding, during-flash, and overall (preceding and/or during-flash) efficiencies. Considering the overall LI detection efficiency (i.e., a flash is counted as detected if it is detected in the preceding and/or during-flash interval), the nighttime efficiency is about 4% higher than the daytime efficiency (78.4% vs. 74.4%). However, when considering during-flash detections only, the nighttime efficiency is higher by about 10%. In contrast, for preceding activity, the detection efficiency is essentially the same for daytime and nighttime.

When considering the analysis outcome, it is also important to keep in mind the following. During the day, negative flashes account for 24 out of 39 events (61.5%), while positive flashes account for 13 events (33.3%) and bipolar flashes for 2 events (5.1%). At night, the dominance of negative polarity is even more pronounced, with 26 out of 37 events (70.3%) classified as negative, compared with 11 positive flashes (29.7%) and no bipolar flashes.

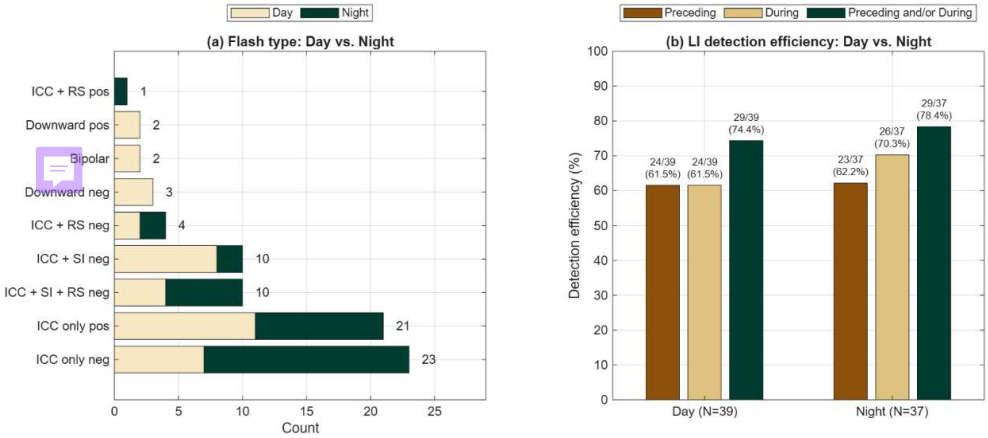

Figure 10 a) Dataset day–night split by flash type: balanced with respect to number of flashes occurring during day and night; b) LI detection efficiency based on the day/night: preceding, during and overall efficiency (preceding and/or during);

Figure 11 shows flash duration versus the number of LGRs in the preceding and during-flash intervals, split by day and night, together with the corresponding day/night median and mean values for the number of LGRs.

For LI LGR detections in the preceding interval, nighttime cases tend to include more detected groups (mean: 75.0 at night vs. 32.0 during the day). Among the five flashes with the highest number of groups in the preceding interval, all are ICC-only flashes: three are positive and two are negative, with the three most intense cases being positive. Four of the top five flashes with the highest number occurred during night.

In contrast, for detections during the flash, the trend is reversed: more LGRs are detected during the day than at night (mean: 44.5 for daytime cases vs. 22.0 for nighttime cases). The three flashes with the highest numbers of during-flash LGRs are associated with RSs, exhibit extreme group counts, and all occurred during the day. Within the top five in terms of number of LI LGRs detected during the flash, all flashes are negative and all occurred during the day. Moreover, the top ten flashes by the number of during-flash LGRs are all negative except for one bipolar case. This is consistent with the dataset, in which negative flashes generally have longer durations than positive flashes, which may help explain why more LGRs are detected for negative flashes than for positive flashes: LI simply has more time to detect groups during longer-lasting negative events. Of the top ten flashes with the highest during-flash LGR counts, only two occurred at night; the remaining eight occurred during the day.

It would generally be expected that LI groups are easier to detect during nighttime because of the lower optical background. Therefore, assuming comparable flash intensity and duration, a larger number of detected groups per flash might be expected at night. However, in this dataset, the opposite tendency is observed for the during-flash interval: both the mean and median number of LGRs are higher for daytime flashes than for nighttime flashes. Inspection of the scatter plot for LI activity during the flash (Figure 11b) indicates that several daytime cases with high numbers of LGRs include RSs or other pulse-type current components. This suggests that the larger number of daytime groups may not be controlled only by the day–night detection conditions, but also by the current structure and optical activity of individual flashes.

https://doi.org/10.5194/egusphere-2026-4653
Preprint. Discussion started: 6 October 2026
© Author(s) 2026. CC BY 4.0 License.

A similar visualization of the day–night dependence of the number of LGRs in the preceding window, restricted to ICC-only flashes and comparing positive and negative ICC-only flashes, is provided in Figure S8 of the Supporting Information.

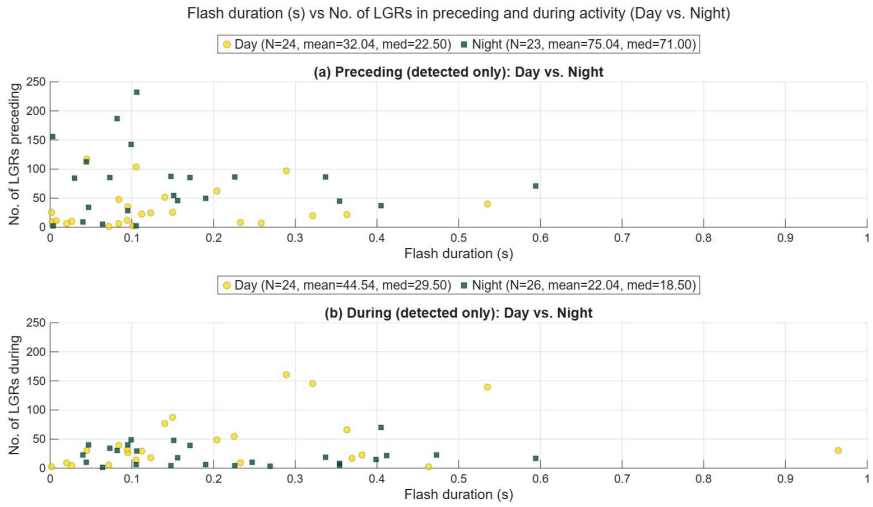

Figure 11 Flash duration versus number of LGRs in the preceding and during-flash intervals, split by day and night.

Furthermore, Figure 12 shows flash duration versus median radiance of LGRs detected in the preceding and during-flash intervals, split by day and night, together with the corresponding mean and median radiance values for daytime and nighttime cases. It must be noted that in the figure the calculated unweighted (by the number of groups) mean and median are determined for unweighted median radiances of particular cases. It should be noted that the mean and median values shown in the figure were calculated as unweighted statistics of the per-event median radiance values, without accounting for the number of detected groups in each event. Nevertheless, when the statistics are weighted by the number of groups per event, the relative relationship between daytime and nighttime radiance remains unchanged. In both the preceding interval and during the flash, the mean and median radiances are approximately 4–5 times higher during the day than those observed at night.

The ten cases with the highest number of LGRs in the preceding interval include positive and negative flashes in roughly equal proportions; however, within the top five preceding-activity cases, four are ICC-only flashes and three of ICC-only flashes are positive and the first with highest radiance value is ICC-only negative. For the cases with the highest radiance during the flash, the top ten comprise five ICC-only flashes and five flashes that also include pulse-type currents (e.g., RSs). Among the top two cases, one includes RSs and one is an SI case, both cases negative; the next three cases are ICC-only. In the top five, four of the cases are negative. Since LI detection is performed after background removal using a threshold that depends on the radiometric noise and background conditions, this daytime enhancement likely reflects the preferential detection of stronger optical signals under higher daytime background illumination.

A similar visualization of the day–night dependence of the median radiance during the current-flow window, restricted to ICC-only flashes and comparing positive and negative ICC-only flashes, is provided in Figure S9 of the Supporting Information.

https://doi.org/10.5194/egusphere-2026-4653
Preprint. Discussion started: 6 October 2026
© Author(s) 2026. CC BY 4.0 License.

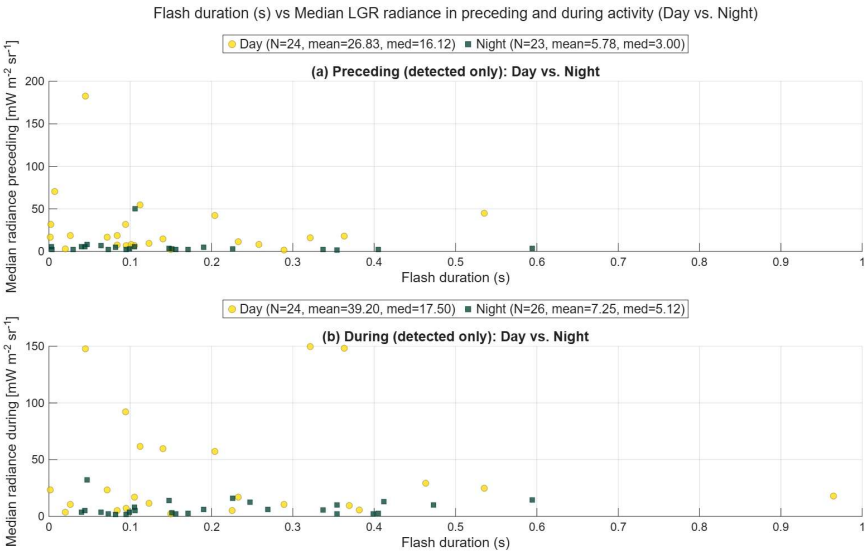

Figure 12 Flash duration versus median radiance in the preceding and during-flash intervals, split by day and night.

4. Flash-level evaluation of LI observations

Here, two representative flashes are analysed to illustrate how LI group timing, location, and radiance relate to the directly measured current waveform and to the LLS context.

4.1 Case 1: Upward Positive Flash with RS

Case 1 occurred on 26 November 2025 at 16:45:19.614 UTC and is classified as a positive flash (ICC + RS) with a total duration of approximately 151 ms. The current measured at the instrumented WT indicated the development of a negative upward leader, and reaches a peak of 15.2 kA. The temporal evolution of the LI detections and the current waveform is summarized in Figure 13, while the spatial distribution of LI groups and LLS detections is shown in Figure 14. A total of 55 LI groups were detected in the 500 ms preceding window and 48 during the flash, with no detections in the post window. The earliest LI detections occur about 0.19 s before the current onset at distances of ~20-25 km, while the closest preceding groups are observed at ~7 km only ~56 ms before the initiation of current at the turbine.

https://doi.org/10.5194/egusphere-2026-4653
Preprint. Discussion started: 6 October 2026
© Author(s) 2026. CC BY 4.0 License.

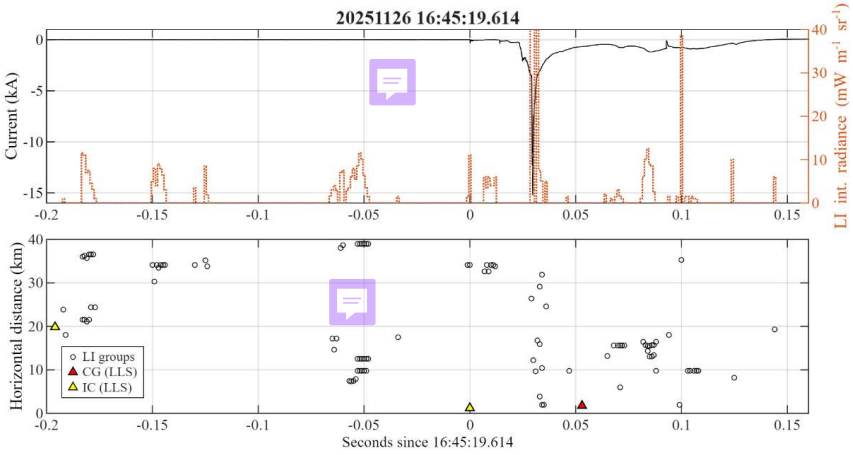

Figure 13. Temporal evolution of Case 1. The upper panel shows the current measured at the wind turbine together with the LI integrated radiance (saturated at 40 $mWm^{-1}sr^{-1}$), while the lower panel shows the distance of LI groups (circles) and LLS detections (triangles) from the turbine as a function of time relative to the current onset. LLS detections are classified as clod-tro-ground strokes (CG) and intra-cloud discharges (IC).

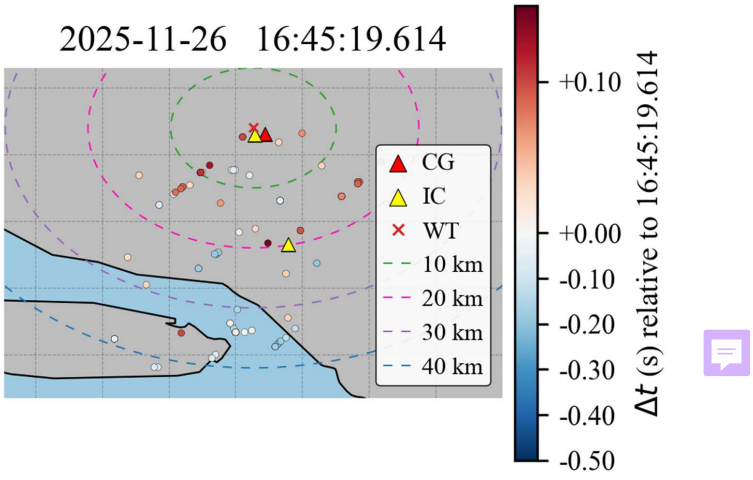

Figure 14. Spatial distribution of LI groups and LLS detections for Case 1. LI groups are color-coded according to their time relative to the current onset, and dashed circles indicate distance from the instrumented wind turbine. Triangles correspond to LLS detections of clod-tro-ground strokes (CG) and intra-cloud discharges (IC).

The spatiotemporal evolution of the LI groups (Figures 14 and 15) reveals a structured development of the parent flash prior to the upward event. The earliest detections coincide with an LLS-classified intracloud discharge (IC) located at ~20 km from the turbine, which is interpreted as the initiation of the parent in-cloud flash system. Following this, LI activity is observed in multiple spatial clusters, initially at distances of 30-40 km and later progressively closer to the turbine, reaching distances below 10 km during the last ~60 ms before current onset. A second IC detection, located at 1.2 km from the turbine and occurring essentially at the onset of the flash, is therefore identified as a likely nearby impulsive process temporally associated with current onset. This sequence is consistent with a lightning-triggered upward flash, in which the first IC establishes the large-scale electrical environment, while the later, nearby IC provides the final perturbation required to initiate the upward negative leader from the structure.

https://doi.org/10.5194/egusphere-2026-4653
Preprint. Discussion started: 6 October 2026
© Author(s) 2026. CC BY 4.0 License.

Once the current is initiated at the turbine, the LI observations show that the most intense optical emission occurs approximately 30 ms after the current onset, simultaneously with the fastest current transition. This delay between electrical and optical maxima is physically significant. It indicates that the initiation of current at the turbine corresponds to the beginning of the upward connection process, whereas the strongest optical emission observed by the satellite is associated with a later and more energetic stage of the flash, likely when the upward negative leader becomes fully connected to the in-cloud discharge and a more luminous process develops in the channel system aloft. The LI groups during this phase exhibit higher radiance, and are predominantly located at distances of ~10-20 km from the turbine, confirming that the satellite primarily observes the luminous in-cloud component of the flash rather than the local attachment process.

Following the main current peak, LI detections continue for several tens of milliseconds, including a secondary radiance maximum around 0.10 s, while the LLS reports a cloud-to-ground (CG) discharge at a location different from the instrumented turbine. This indicates that, after the upward leader from the turbine was triggered and the main current pulse occurred, the parent flash system remained active and continued to evolve elsewhere within the cloud and/or at another attachment point. Therefore, this case is best interpreted as a triggered upward flash embedded within a larger and spatially extended flash system, rather than an isolated discharge confined to the turbine.

4.2 Case 2: Upward Negative Flash with Return Stroke

Case 2 occurred on 25 January 2026 at 11:09:17.920 UTC and is classified as an ICC + SI + RS negative flash, with a total duration of about 965 ms. In contrast to Case 1, no LI groups were detected in the 500 ms preceding window, and no IC or CG discharges were reported by the LLS within 50 km before the onset of the current at the instrumented WT. During the flash, however, 30 LI groups were detected. The temporal evolution shown in Figure 15 indicates that the first LI detections occur only after the flash has already started. This behavior immediately suggests that the optical activity becomes visible only once the flash is more fully developed aloft.

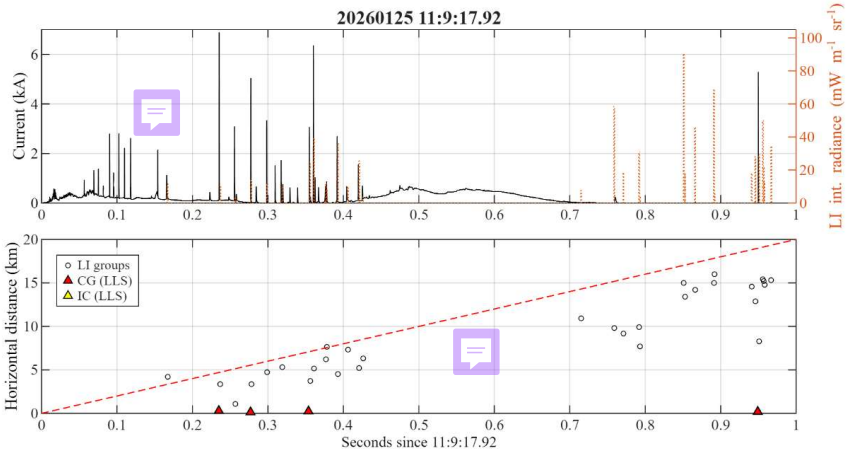

Figure 15. Temporal evolution of Case 2. The upper panel shows the current measured at the wind turbine together with the LI integrated radiance, while the lower panel shows the distance of LI groups and LLS detections from the turbine as a function of time relative to the current onset. The red dashed line indicates the expected distance-time trend for a typical positive leader speed.

The absence of both LI and LLS detections prior to the measured current makes this event a candidate for self-initiated upward lightning. At the same time, this interpretation should be stated carefully. The flash occurred around local noon in Croatia, when the solar background is high, and this can reduce LI sensitivity to weaker optical emissions. Therefore, the lack of preceding LI activity does not strictly prove that no in-cloud discharge occurred before the flash. Nevertheless, the simultaneous absence of any preceding LLS-classified IC or CG activity within 50 km is highly remarkable and is consistent with, but does not prove, self-initiation hypothesis. Taken together, that would be consistent with a situation in which the ambient thunderstorm electric field above the wind turbine became sufficiently strong to launch an upward leader directly from the structure, without any

https://doi.org/10.5194/egusphere-2026-4653
Preprint. Discussion started: 6 October 2026
© Author(s) 2026. CC BY 4.0 License.

clearly detectable nearby triggering flash. In that sense, Case 2 appears fundamentally different from triggered cases, where preceding in-cloud discharges can be identified and linked to the onset of the upward flash.

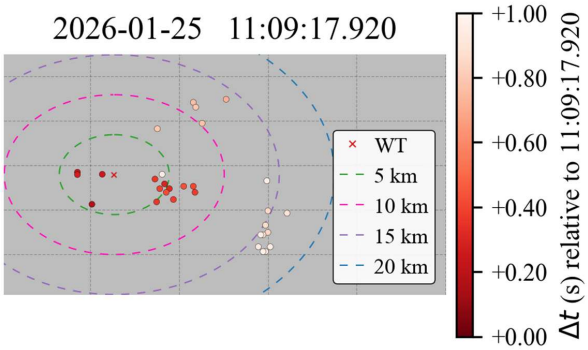

Figure 16. Spatial distribution of LI groups for Case 2. LI groups are color-coded according to their time relative to the current onset, and dashed circles indicate distance from the wind turbine.

Once the current starts, the LI detections form a compact and organized spatiotemporal pattern, as shown in Figure 15 and 16. The groups are confined to distances of only a few kilometers from the turbine during the first detected optical stage and then progressively extend outward with time, from roughly 1-8 km in the earlier part of the LI sequence to about 10-16 km later in the flash. The time-distance plot suggests an apparent propagation compatible, at least in order of magnitude, with the reference positive-leader-speed line shown in the figure (red dashed line). Thus, the LI observations may be interpreted as the cloud-top luminous manifestation of the upward-flash development after initiation, as the leader system extends away from the structure and the connected channel system becomes increasingly luminous. This interpretation is also consistent with the spatial map, where the LI groups remain concentrated around the turbine rather than being distributed over tens of kilometers.

The current waveform and LI radiance sequence further indicate that the flash becomes optically active only after initiation and then evolves through several luminous bursts. In Figure 15, multiple LI radiance peaks occur during the interval in which the current waveform exhibits repeated pulse-type activity superimposed on the longer current flow. Four CG detections are reported by the LLS during this same interval, at times that coincide with the LI activity. This suggests that, after the self-initiated upward leader was launched from the turbine, the flash evolved into a more complex discharge containing stroke-type processes and repeated luminous activity in the cloud. The late LI detections, including the strong pulses near the end of the current record and the post-window group immediately after flash termination, indicate that the flash system remained optically active until the final stage of the event.

5. Conclusions

This paper presents the first systematic evaluation of Meteosat-12 Lightning Imager observations using direct current measurements of lightning flashes striking a tall structure at a site dominated by upward lightning activity. Tall tower upward lightning differs fundamentally from natural downward cloud-to-ground lightning, particularly during its initiation phase. Upward flashes begin with the development of an upward leader and are characterized by a low-frequency, long-duration ICC, which may subsequently be followed by one or more RSs and CCs. In contrast, in natural downward cloud-to-ground lightning, an RS occurs immediately after the downward leader connects with a UCL initiated from the ground or a grounded object and may subsequently be followed by a CC. In this context, the observatory provides a valuable dataset for validating LI observations of upward lightning and assessing the instrument's ability to detect the optical signatures associated with a wide range of current components occurring within a flash, from low-frequency, long-duration currents such as ICC and CC to high-frequency, pulse-type components such as RSs and ICC pulses.

Concretely, in this work we utilize an instrumented wind turbine in Croatia as the primary reference. The analyzed dataset comprises 76 current waveforms recorded during an 18-month measurement campaign, extending from July 2024, when Meteosat-12 began disseminating data, through February 2026. Specifically, the LI Group (LGR) product was used in the analysis.

https://doi.org/10.5194/egusphere-2026-4653
Preprint. Discussion started: 6 October 2026
© Author(s) 2026. CC BY 4.0 License.

The results demonstrated an overall LI flash detection efficiency of 76.3% when detections occurring either during the preceding-activity window or during the measured current-flow window were considered. The corresponding detection efficiencies were 61.8% for preceding activity and 65.8% during the measured current flow. These findings demonstrate that the LI onboard Meteosat-12 detects a substantial fraction of wind-turbine lightning cases, including flashes containing continuing-current processes such as ICCs and CCs. This capability is particularly important because ground-based lightning location systems often have limited ability to detect ICCs and CCs. Upward flashes may consist solely of an initial ICC phase, and at some instrumented sites, ICC-only flashes account for approximately 40–50% of all upward flashes. Consequently, relying exclusively on LLS observations may lead to a substantial underestimation of lightning occurrence and the associated risk at tall structures.

The main conclusions can be grouped into two categories: (a) conclusions related to the detection efficiency of the LI and its preferential detection characteristics with respect to lightning polarity, flash type, and daytime/nighttime conditions, providing a foundation for a better understanding of the underlying lightning initiation and development processes within the cloud structure; and (b) potential applications of the LI in power systems, implied by and supported by the evidence presented in this measurement campaign.

5.1 Detection Characteristics of the Lightning Imager with Respect to Polarity, Flash Type, and Day/Night Conditions

A key result is that the preceding and during-current windows provide different observational information. LI detections before the onset of current at the turbine indicate that a large fraction of the cases were associated with optical activity occurring before the measured current began, consistent with nearby or parent in-cloud lightning activity that may contribute to upward-flash initiation. However, the absence of preceding-window LI detections should not be interpreted as definitive evidence of self-initiation, since weak, obscured, or optically attenuated in-cloud activity may remain below the LI detection threshold. During the during-current window, LI detectability is more strongly affected by the current waveform structure, especially the presence of pulse-type components such as RSs or pulses superimposed on continuing current, which are associated with stronger optical emissions.

The statistical analysis shows that LI performance also depends on the polarity of the flash. In the during-current window, positive and negative flashes are essentially the same, with more than half of each subset detected; this also holds true when comparing ICC-only positive and ICC-only negative flashes, thereby eliminating the potential impact of impulsive phases such as RSs and allowing us to isolate the pure polarity effect on detection. In the preceding window, however, positive flashes, particularly ICC-only positive flashes, exhibited higher detection efficiency than negative flashes in this dataset. This can be explained by the fact that the triggering mechanism in positive cases occurs near the upper main charge region inside the cloud.

Furthermore, negative flashes generally showed larger median LGR counts, especially in the during-current window, consistent with their longer average duration.

Radiance statistics of the detected LGRs indicate that the higher radiance of negative flashes in the during-current window in the full dataset is strongly influenced by cases with pulse-type current components. Within the ICC-only subset, positive flashes showed higher median radiance than negative flashes, suggesting that LI response for continuing-current-dominated flashes depends not only on the measured current at the turbine, but also on the broader optical development of the associated cloud discharge.

The day/night analysis indicates that nighttime conditions slightly improve overall and during-current-window detection efficiency, as expected since background optical noise is lower. However, the number of detected LGRs and the radiance statistics are not controlled by day/night conditions alone. Several daytime negative flashes with long durations and pulse-type current components dominate the during-current-window LGR counts, while daytime median radiances are higher because LI thresholding under stronger background illumination preferentially retains stronger optical signals. Therefore, flash type, current structure, duration, and polarity can dominate over the simple day/night background effect.

The flash-level analysis further illustrates how LI observations relate to the directly measured current waveform and to the LLS context. The selected cases represent two contrasting situations: one upward flash with clear preceding LI activity before current onset, and one upward flash with no preceding LI or LLS detections within the analysis window. These examples show that LI generally observes the cloud-top optical manifestation of the broader lightning process rather than the local attachment process alone. Consequently, combining LI group timing, radiance, distance, LLS detections, and directly measured current waveforms provides a physically grounded approach for interpreting what LI observes during wind-turbine lightning events.

Finally, the results should be interpreted considering the relatively limited number of cases in each flash class and the fact that the dataset comes from a single instrumented wind turbine in a winter-lightning region. Therefore, the observed polarity- and flash-type-dependent tendencies should be regarded as characteristics of this dataset

https://doi.org/10.5194/egusphere-2026-4653
Preprint. Discussion started: 6 October 2026
© Author(s) 2026. CC BY 4.0 License.

rather than as general conclusions for all upward lightning. Future detailed meteorological analysis is needed to confirm storm type and further interpret these results. This could include classifying the illuminated cloud regions as convective, stratiform, mixed, or non-raining/boundary, as well as determining the cloud optical depth. Applying this to cases where positive flashes were detected versus not detected, and similarly for negative flashes, would help establish whether the observed polarity-dependent detection differences are driven by storm type and cloud optical thickness rather than by charge-region depth alone.

Nevertheless, the study demonstrates the value of direct lightning-current measurements for evaluating satellite optical lightning observations and provides a reference methodology for future assessments of Meteosat-12 LI performance for upward lightning and continuing-current-dominated flashes.

5.2 Implications of the Lightning Imager for Power-System Applications

The combined satellite and ground-based observations presented in this study highlight two characteristics of LI measurements that may be relevant both for lightning research and for operational applications involving power-system infrastructure.

First, LI detected optical emissions associated with several intense return strokes and provided spatial information on the corresponding lightning activity. Such observations may complement measurements from ground-based lightning location systems when investigating the relationship between lightning and faults or interruptions in overhead transmission networks. In particular, the combined use of satellite and ground-based observations could support the attribution of power-system events to nearby lightning activity, although the suitability of LI for operational fault attribution will also depend on its detection efficiency, spatial uncertainty, temporal sampling, and the characteristics of the lightning event.

Second, LI provides sequences of optical observations that may extend beyond impulsive return-stroke emissions and include portions of the initial and subsequent continuing-current phases. These processes often go undetected by operational LLSs, demonstrating the significant added value of LI detections. The accumulated radiance of the LI groups associated with a flash may therefore provide information on the relative duration and optical output of the flash. Although satellite-observed radiance cannot be interpreted directly as the electrical energy transferred by the lightning current, it may serve as an observational indicator of differences among flashes when interpreted together with current measurements and other ground-based observations. Over longer observation periods, such information could contribute to identifying areas where infrastructure is repeatedly exposed to optically intense or long-duration lightning activity.

These potential applications require further validation using larger datasets and a broader range of lightning conditions. Nevertheless, the results indicate that LI observations may provide complementary information on both impulsive and continuing lightning processes that is not always available from conventional lightning location measurements alone.

Data availability

All raw data can be provided by the corresponding authors upon request.

Author contribution

FV, JM, MA and BFG planned the campaign; FV and BFG performed the ground-based current measurements; FV, JM, MA collected and analyzed the data associated with LI; FV and MA wrote the manuscript draft; FV, JM, MA and BFG reviewed and edited the manuscript.

Competing interests

The authors declare that they have no conflict of interest.

Acknowledgement

This research is carried out and financed within the framework of the second Swiss Contribution MAPS. *Grant number IZ11Z0_230951*: WISE - Wind turbine lightning safety evaluation is funded by the Swiss National Science Foundation (SNSF) and the Croatian Science Foundation (HRZZ). This work was also supported by research Grants PID2025-173955OA-I00, PID2025-169163NB-C32, PID2022-136348NB-C32 and EQC2021-006957-P funded by MCIN/AEI/10.13039/501100011033, and by "ERDF A way of making Europe", by the "European Union".

https://doi.org/10.5194/egusphere-2026-4653
Preprint. Discussion started: 6 October 2026
© Author(s) 2026. CC BY 4.0 License.

References

Blakeslee, R. J., Lang, T. J., Koshak, W. J., Buechler, D., Gatlin, P., Mach, D. M., Stano, G. T., Virts, K. S., Walker, T. D., Cecil, D. J., Ellett, W., Goodman, S. J., Harrison, S., Hawkins, D. L., Heumesser, M., Lin, H., Maskey, M., Schultz, C. J., Stewart, M., Bateman, M., Chanrion, O., and Christian, H.: Three years of the Lightning Imaging Sensor onboard the International Space Station: Expanded global coverage and enhanced applications, J. Geophys. Res.-Atmos., 125, e2020JD032918, https://doi.org/10.1029/2020JD032918, 2020.

Bližňák, V. and Sokol, Z.: First validation of the Lightning Imager aboard Meteosat Third Generation satellite with Earth Networks Total Lightning Network, Int. J. Appl. Earth Obs. Geoinf., 147, 105205, https://doi.org/10.1016/j.jag.2026.105205, 2026.

Boccippio, D. J. and Christian, H. J.: Optical detection of lightning from space, NASA Technical Report, NASA Marshall Space Flight Center, Huntsville, Alabama, USA, NASA NTRS Document ID 19990008509, 1998.

Christian, H. J., Blakeslee, R. J., Buechler, D. E., Koshak, W. J., Driscoll, K. T., and Mach, D. M.: The Lightning Imaging Sensor, in: Proceedings of the 11th International Conference on Atmospheric Electricity, Guntersville, Alabama, USA, NASA Conference Publication NASA/CP-1999-209261, 746–749, 1999.

CIGRE Working Group C4.407: Lightning Parameters for Engineering Applications, CIGRE Technical Brochure 549, CIGRE, Paris, France, 118 pp., 2013.

Dobber, M. and Grandell, J.: Meteosat Third Generation (MTG) Lightning Imager (LI) instrument performance and calibration from user perspective, in: Proceedings of the 23rd Conference on Characterization and Radiometric Calibration for Remote Sensing (CALCON), Logan, Utah, USA, 11–14 August 2014, 13 pp., 2014.

Enno, S.-E., Viticchié, B., Navia, D., and Grandell, J.: Meteosat-12 Lightning Imager: First year of observations and the main performance characteristics, 12th European Conference on Severe Storms, Utrecht, the Netherlands, 17–21 November 2025, ECSS2025-152, https://doi.org/10.5194/ecss2025-152, 2025.

Erdmann, F., Defer, E., Caumont, O., Blakeslee, R. J., Pédeboy, S., and Coquillat, S.: Concurrent satellite and ground-based lightning observations from the Optical Lightning Imaging Sensor (ISS-LIS), the low-frequency network Meteorage, and the SAETTA Lightning Mapping Array (LMA) in the northwestern Mediterranean region, Atmos. Meas. Tech., 13, 853–875, https://doi.org/10.5194/amt-13-853-2020, 2020.

Figueras i Ventura, J., Pineda, N., Besic, N., Grazioli, J., Hering, A., van der Velde, O. A., Romero, D., Šunjerga, A., Mostajabi, A., Azadifar, M., Rubinstein, M., Montanyà, J., Germann, U., and Rachidi, F.: Polarimetric radar characteristics of lightning initiation and propagating channels, Atmos. Meas. Tech., 12, 2881–2911, https://doi.org/10.5194/amt-12-2881-2019, 2019.

Gedik, E., Mansouri, E., Kohlmann, H., Schulz, W., and Rubinstein, M.: Performance evaluation of Meteosat Third Generation Lightning Imager in detecting lightning discharges, in: Proceedings of the XVIII International Symposium on Lightning Protection (SIPDA 2025), Thessaloniki, Greece, 21–26 September 2025, 1–5, https://doi.org/10.1109/SIPDA68639.2025.11296657, 2025.

Goodman, S. J., Blakeslee, R. J., Koshak, W. J., Mach, D., Bailey, J., Buechler, D., Carey, L., Schultz, C., Bateman, M., McCaul, E., and Stano, G.: The GOES-R Geostationary Lightning Mapper (GLM), Atmos. Res., 125–126, 34–49, https://doi.org/10.1016/j.atmosres.2013.01.006, 2013.

Holmlund, K., Grandell, J., Schmetz, J., Stuhlmann, R., Bojkov, B., Munro, R., Lekouara, M., Coppens, D., Viticchié, B., August, T., Theodore, B., Watts, P., Dobber, M., Fowler, G., Bojinski, S., Schmid, A., Salonen, K., Tjemkes, S., Aminou, D., and Blythe, P.: Meteosat Third Generation (MTG): Continuation and innovation of observations from geostationary orbit, B. Am. Meteorol. Soc., 102, E990–E1015, https://doi.org/10.1175/BAMS-D-19-0304.1, 2021.

https://doi.org/10.5194/egusphere-2026-4653
Preprint. Discussion started: 6 October 2026
© Author(s) 2026. CC BY 4.0 License.

Holmlund, K., Counet, P., Martinez Fadrique, F., Schmid, A., Bojkov, B., Munro, R., Grandell, J., and Obligis, E.: The EUMETSAT satellite programmes and data services, J. Eur. Meteorol. Soc., 2, 100005, https://doi.org/10.1016/j.jemets.2024.100005, 2025.

Hui, W., Zhang, W., Lyu, W., and Li, P.: Preliminary observations from the China Fengyun-4A Lightning Mapping Imager and its optical radiation characteristics, Remote Sens., 12, 2622, https://doi.org/10.3390/rs12162622, 2020.

IEC: IEC 61400-24:2019, Wind energy generation systems – Part 24: Lightning protection, International Electrotechnical Commission, Geneva, Switzerland, 2019.

Montanyà, J., van der Velde, O., and Williams, E. R.: Lightning discharges produced by wind turbines, J. Geophys. Res.-Atmos., 119, 1455–1462, https://doi.org/10.1002/2013JD020225, 2014.

Montanyà, J., van der Velde, O. A., Romero, D., March, V., Solà, G., Pineda, N., Arrayás, M., Trueba, J. L., Reglero, V., and Neubert, T.: A simultaneous observation of lightning by ASIM, Colombia-Lightning Mapping Array, GLM, and ISS-LIS, J. Geophys. Res.-Atmos., 126, e2020JD033735, https://doi.org/10.1029/2020JD033735, 2021.

Montanyà, J., López, J. A., van der Velde, O. A., Romero, D., Solà, G., Pineda, N., and Arcanjo, M.: Potential use of space-based lightning detection in electric power systems, Electr. Pow. Syst. Res., 213, 108730, https://doi.org/10.1016/j.epsr.2022.108730, 2022.

Poelman, D. R. and Schulz, W.: Comparing lightning observations of the ground-based European lightning location system EUCLID and the space-based Lightning Imaging Sensor (LIS) on the International Space Station (ISS), Atmos. Meas. Tech., 13, 2965–2977, https://doi.org/10.5194/amt-13-2965-2020, 2020.

Rachidi, F. and Rubinstein, M.: Säntis lightning research facility: A summary of the first ten years and future outlook, Elektrotech. Inftech., 139, 379–394, https://doi.org/10.1007/s00502-022-01031-2, 2022.

Rakov, V. A. and Uman, M. A.: Lightning: Physics and Effects, Cambridge University Press, Cambridge, UK, 687 pp., 2003.

van der Velde, O. A., Montanyà, J., Neubert, T., Chanrion, O., Østgaard, N., Goodman, S., and Christian, H.: Comparison of high-speed optical observations of a lightning flash from space and the ground, Earth Space Sci., 7, e2020EA001249, https://doi.org/10.1029/2020EA001249, 2020.

Viticchié, B., Enno, S.-E., Navia, D., Avbelj, J., and Grandell, J.: Meteosat Third Generation Lightning Imager detection performances, EGUsphere [preprint], https://doi.org/10.5194/egusphere-2026-3177, 2026.

Vuković, F., Filipović-Grčić, B., Stipetić, N., and Franc, B.: Installation and initial measurement results of the Rogowski-coil-based wind turbine lightning current waveform measurement system, Electr. Pow. Syst. Res., 238, 111061, https://doi.org/10.1016/j.epsr.2024.111061, 2025a.

Vuković, F., Montanyà, J., and Filipović-Grčić, B.: Observing lightning on a wind turbine in Croatia: Ground-based measurements and Lightning Imager radiance, in: Proceedings of the XVIII International Symposium on Lightning Protection (SIPDA 2025), Thessaloniki, Greece, 21–26 September 2025, 1–6, https://doi.org/10.1109/SIPDA68639.2025.11296687, 2025b.

Vuković, F., Filipović-Grčić, B., Stipetić, N., and Franc, B.: Electromagnetic transients and failed upward leaders observed during lightning activity in an onshore wind farm, Electr. Pow. Syst. Res., 251, 112216, https://doi.org/10.1016/j.epsr.2025.112216, 2026a.

Vuković, F., Montanyà, J., and Filipović-Grčić, B.: Lightning flash observations on a wind turbine in Croatia: Insights from current measurements, high-speed camera, LLS and lightning imager data, Electr. Pow. Syst. Res., 251, 112315, https://doi.org/10.1016/j.epsr.2025.112315, 2026b.